Mathematics Interdisciplinary Research **9** (1) (2024) 1 − 22

Original Scientific Paper

Virtual Element Method for Numerical Simulation of Burgers-Fisher Equation on Convex and Non-Convex Meshes

Allahbakhsh Yazdani Cherati⋆ and Hamid Momeni

Abstract

We present an enhanced approach to solving the combined non-linear time-dependent Burgers-Fisher equation, which is widely used in mathematical biology and has a broad range of applications. Our proposed method employs a modified version of the finite element method, specifically the virtual element method, which is a robust numerical approach. We introduce a virtual process and an Euler-backward scheme for discretization in the spatial and time directions, respectively. Our numerical scheme achieves optimal error rates based on the degree of our virtual space, ensuring high accuracy. We evaluate the efficiency and flexibility of our approach by providing numerical results on both convex and non-convex polygonal meshes. Our findings indicate that the proposed method is a promising tool for solving non-linear time-dependent equations in mathematical biology.

Keywords: Virtual element method, Burgers-Fisher equation, Convex mesh, Non-convex mesh, Non-linearity.

2020 Mathematics Subject Classification: 65M15, 65M25, 65M50.

How to cite this article
A. Yazdani Cherati and H. Momeni, Virtual element method for numerical simulation of Burgers-Fisher equation on convex and non-convex meshes, *Math. Interdisc. Res.* **9** (1) (2024) 1–22.

⋆Corresponding author (E-mail: yazdani@umz.ac.ir)
Academic Editor: Akbar Mohebbi
Received 16 April 2023, Accepted 25 October 2023
DOI: 10.22052/MIR.2023.252806.1403

1. Introduction

In this paper, we seek an approximate solution for the Burgers-Fisher equation under the initial and Direchlet boundary conditions presented below: for $(\mathbf{x}, t) \in \Omega \times [0, T]$

$$u_t(\mathbf{x}, t) - \Delta u(\mathbf{x}, t) - \alpha u(\mathbf{x}, t)\nabla \cdot u(\mathbf{x}, t) + u(\mathbf{x}, t)(1 - u(\mathbf{x}, t)) = 0, \tag{1}$$

$$u(\mathbf{x}, 0) = u^0(\mathbf{x}), \quad \mathbf{x} \in \Omega, \tag{2}$$

$$u(\mathbf{x}, t) = u^{\partial}(\mathbf{x}, t), \quad (\mathbf{x}, t) \in \partial\Omega \times (0, T]. \tag{3}$$

The spatial domain Ω is a subset of $\mathbb{R}^d$, where d can be 1, 2, or 3. The term u_t represents the time derivative of the function u. The Laplacian operator is well-defined as $\Delta = \partial^2_{x_1} + \cdots + \partial^2_{x_d}$. The initial data u^0 and boundary data u^{∂} are given functions that specify the initial and boundary conditions for the exact solution u, respectively.

For the model problem (1)-(3) the weak formulation can form as: find $u(\mathbf{x}, t) \in L^2(0, T; H^1(\Omega))$ such that

$$\begin{cases} (u_t, v) + a(u, v) = (f(u), v), & \text{for} \quad v \in H^1_0(\Omega), \\ u(\mathbf{x}, 0) = u^0(\mathbf{x}), & \mathbf{x} \in \Omega, \end{cases} \tag{4}$$

where $f(u) = \alpha u \nabla \cdot u - u(1 - u)$, $(\cdot, \cdot)$ is the usual L^2 inner-product and $a(\cdot, \cdot)$ is the grad-grad H^1 inner-product of two functions.

The model equation (1) has a highly non-linear nature due to the presence of diffusion, convection, and reaction mechanisms in its formulation. When $\alpha = 0$, we have the well-known Fisher's equation. This equation was introduced by Fisher in [1] to describe the population dynamics to investigate the dispersion of a mutant gene.

Partial differential equations (PDEs) as one of the fundamental tools in mathematical modeling and analysis, are used to describe various physical phenomena in fields such as physics, engineering, biology, and finance. Studying and analyzing the behavior of these equations allows scientists and researchers to gain a deeper understanding of these phenomena. By studying equations, they can uncover patterns, make predictions, and develop mathematical models that can be used to solve real-world problems. In some cases, the lack of an analytical solution or the time required to obtain such a solution leads researchers to use numerical methods to approximate solutions.

Various numerical methods for approximating the solution of PDEs have been developed in recent years. By discretizing the PDEs into a system of algebraic equations, these methods aim to provide efficient and accurate approximations. Finite difference [2], finite element [3, 4], and finite volume [5] methods are some of the most commonly used numerical methods. These techniques have been used successfully in a variety of fields, including fluid dynamics, structural analysis,

and electromagnetic simulations. Furthermore, advances in computational power have enabled the development of more sophisticated numerical methods capable of dealing with complex geometries and non-linear problems.

Meshing the computational domain into an arbitrary number of elements (such as polygons or polyhedrons) is a common approach used in numerical simulations and computational modeling. This process, known as mesh generation, allows for the accurate representation of complex geometries and facilitates the analysis of the solution of PDEs on these domains. Among the mesh-generation based methods, the virtual element method (VEM) is a promising technique that has gained attention in recent years [6–10]. The VEM combines the advantages of finite element methods (FEM) and mimetic finite difference methods [11, 12], allowing for the accurate approximation of solutions on arbitrary polygonal or polyhedral meshes. It provides a versatile framework for tackling a wide range of problems, including those with complex geometries. The most important feature of the VEM is its mathematical foundation, which allows it to approximate the solution to the problem in a simpler manner than the FEM. Additionally, the VEM offers greater flexibility in terms of incorporating different types of elements, such as convex and non-convex, which further enhances its applicability in various engineering and scientific domains. The weak formulation of the model problem serves as the foundation for both FEM and VEM. Contrary to the FEM, the VEM does not necessitate computing the explicit computation of the shape functions on a polygon. Based on the weak formulation (4) of the model problem (1)-(3), due to the inclusion of the grad-grad term in this formulation, integrals of the gradient of the shape functions may need to be computed in order to form the element matrices using a quadrature formula on the corresponding element. Also, the FEM may encounter difficulties as a result of the non-linearity term's presence. On the other hand, the VEM can deal with these difficulties in a simpler way.

The first steps in developing this numerical method can be traced back to paper [13], which introduced VEM as a generalization of FEM. Since then, VEM has been applied to a wide range of problems and many efforts have been made to develop this numerical method. In [14], the practical aspects of VEM for the Poisson equation in two and three dimensions are investigated. The numerical approximations for semi-linear parabolic problems based on conforming VEM have been studied in [15]. In [16], a non-conforming VEM for the approximation of the time-fractional reaction-subdiffusion equation has been investigated. A unified framework is introduced to study the conforming and non-conforming VEMs for a class of time-dependent fourth-order reaction-subdiffusion equations with the Caputo derivative in [17].

The primary objective of VEM is to establish an optimal and efficient way in order to compute the integrals based on discrete bilinear forms, where two projection operators Π^{∇} and Π^{0} are defined to discretize the grad-grad term and the term that involved time derivatives, respectively. We demonstrated how the non-linearity term can be handled differently when using the defined projection operator Π^{0}. The validity of the theoretical findings is demonstrated by numerical

outcomes, which also demonstrate the precision of the calculations. Researchers can confidently conclude this data and make reasoned decisions.

Throughout this paper, for $1 \leq p < \infty$ and $k \geq 0$ we adopt the following notation on Ω

$$\|\cdot\|_{L^p(0,T;H^s(\Omega))} = \Big(\int_0^T |\cdot|_k^p \, ds \Big)^{1/p},$$

where $\|\cdot\|_{L^P}$ is the usual L^p-norm and $|\cdot|_k = |\cdot|_{H^k(\Omega)}$ is the semi-norm defined in the Sobolev space $H^k(\Omega)$.

2. Discrete schemes

Assume that $\mathcal{T}_h$ represents the partition of the spatial domain $\Omega \subset \mathbb{R}^2$. For any given element $E \in \mathcal{T}_h$, we define h as the maximum diameter among all elements $E \in \mathcal{T}_h$, denoted by h_E. The set of edges of $\mathcal{T}_h$ is denoted by $\mathcal{E}_h$ where we define $\mathcal{E}_0$ and $\mathcal{E}_b$ to be the interior and boundary of edges, respectively. As with traditional ways for the FEM family, to formulate discrete schemes for a model problem, we need to introduce our local and global computational space. To achieve this goal, first we need to introduce some essential instruments for our algorithm. Let E be an arbitrary element. We introduce the local function space V_h^E as follows:

$$V_h^E := \{v_h \in H^1(E) \cap C^0(\partial E) : \Delta v_h \in \mathbb{P}_{k-2}(E),\ v_h|_e \in \mathbb{P}_k(E),\ \forall e \in \partial E\}, \quad (5)$$

where $\mathbb{P}_k(E)$ is the space of polynomial of degree less than or equal to k. As a conventional way for VEM, it should be noted here that a function v_h in the local space V_h^E can identify by

- The values of v_h at k vertices of element E,
- For $k \geq 2$, the values of v_h at $k-1$ distinct points on each edge e,
- The moments $\frac{1}{|E|}\int_E v_h\, p$, for $p \in \mathbb{P}_{k-2}(E)$.

Based on the weak formulation (4), we define the following notations

$$\begin{aligned} a(u,v) &:= \sum_{E\in\mathcal{T}_h} a^E(u,v), \\ (u,v) &:= \sum_{E\in\mathcal{T}_h} (u,v)_E. \end{aligned} \quad (6)$$

Next, we define our projection operators Π^0 and Π^∇ on space V_h^E.

- The projector operator $\Pi^{\nabla} : V_h^E \to \mathbb{P}_k(E)$ is defined by

$$\begin{cases} a^E(\Pi^{\nabla} v_h, p) = a^E(v_h, p), & \text{for} \quad p \in \mathbb{P}_k(E), \\ P_0(\Pi^{\nabla} v_h) = P_0 v_h, & \text{for} \quad v_h \in V_h^E, \end{cases}$$

  and

$$P_0 v_h := \frac{1}{n_v} \sum_{i=1}^{n_v} v_{h,i}, \quad \text{for} \quad k = 1,$$
$$P_0 v_h := \frac{1}{|E|} \int_E v_h \, dx, \quad \text{for} \quad k > 1,$$

  where n_v denotes the vertices of an element E and $v_{h,i}$ denotes the value of v_h at the i-th degree of freedom in V_h^E.

- The standard L^2-projection operator $\Pi^0 : V_h^E \to \mathbb{P}_k(E)$ will introduce as

$$(\Pi^0 v_h - v_h, p)_E = 0, \quad \forall p \in \mathbb{P}_k(E), \ v_h \in V_h^E.$$

Ultimately, we can define our local and global virtual element space by utilizing the aforementioned projection operators in the following manner:

$$W_h(E) := \{v_h \in V_h^E : \int_E (\Pi^{\nabla} v_h) \, p \, d\mathbf{x} = \int_E (v_h) \, p \, d\mathbf{x}, \, \forall \, p \in \mathbb{P}_k \backslash \mathbb{P}_{k-2}\},$$

and

$$W_h := \{v_h \in H^1(\Omega) : v_h|_E \in W_h(E), \, \forall E \in \mathcal{T}_h\}.$$

For those who are interested in further details regarding the construction of the projection operators and corresponding spaces, we recommend consulting [13, 14].

Following [18], to formulate our semi and fully-discrete schemes, we first improve our bilinear forms defined in (6). For the local discrete bilinear forms $(\cdot, \cdot)_{h,E} : W_h(E) \times W_h(E) \to \mathbb{R}$ and $a_h^E : W_h(E) \times W_h(E) \to \mathbb{R}$, we define our global bilinear forms as follows:

$$a_h(u, v) = \sum_{E \in \mathcal{T}_h} a_h^E(u, v),$$
$$(u, v)_h = \sum_{E \in \mathcal{T}_h} (u, v)_{h,E}, \quad \text{for} \quad u, v \in W_h.$$

Based on the defined projection operators, the local bilinear forms will be defined as:

$$a_h^E(u_h, v_h) := a^E(\Pi^{\nabla} u_h, \Pi^{\nabla} v_h) + S_a^E((I - \Pi^{\nabla})u_h, (I - \Pi^{\nabla})v_h), \tag{7}$$
$$(u_h, v_h)_{h,E} := (\Pi^0 u_h, \Pi^0 v_h)_E + S^E((I - \Pi^0)u_h, (I - \Pi^0)v_h), \quad \forall \, u_h, v_h \in W_h(E), \tag{8}$$

where, S_a^E and S^E are the symmetric stabilizing terms for our algorithm.

Based on the definition for the two bilinear forms, we consider the following properties for them:

- *consistency*: on each element $E \in \mathcal{T}_h$, for all $p \in \mathbb{P}_k(E)$ and $v \in W_h(E)$, we have

$$a_h^E(p, v) = a^E(p, v),$$
$$(p, v)_{h,E} = (p, v)_E,$$

- *stability*: for all $v \in W_h(E)$ and some positive constants $\alpha_*, \alpha^*, \beta_*$ and β^*, independent of h,

$$\alpha_* a^E(v, v) \leq a_h^E(v, v) \leq \alpha^* a^E(v, v),$$
$$\beta_*(v, v)_E \leq (v, v)_{h,E} \leq \beta^*(v, v)_E. \tag{9}$$

Now we have all the necessary tools, and can define our semi-discrete scheme for the continuous problem (1)-(3) to find $u_h \in L_2(0, T; W_h)$ such that

$$\begin{cases} (\partial_t u_h, v_h)_h + a_h(u_h, v_h) = (\tilde{f}(u_h(\cdot, t)), v_h), \forall v_h \in W_h, \\ u_h(\cdot, 0) = u_h^0, \end{cases} \tag{10}$$

where u_h^0 and $\tilde{f}$ are approximations of u^0 and f, respectively.

Let the function space W_h has a total of N^{dof} degrees of freedom. The bilinear forms $a_h(\cdot, \cdot)$ and $(\cdot, \cdot)_h$ satisfy symmetry and stability conditions, from which it can be shown that the problem (10) has a unique solution as [18]:

$$u_h(t) := \sum_{n=1}^{N^{dof}} \left((u_h^0, w_h^{(n)})_h e^{-\lambda_h^{(n)} t} + \int_0^t (\tilde{f}(u_h(\cdot, s)), w_h^{(n)}) e^{-\lambda_h^{(n)}(t-s)} \, ds \right) w_h^{(n)},$$

where $\{\lambda_h^{(n)}\}_{n=1}^{N^{dof}}$ is a set of strictly positive constants and $\{w_h^{(n)}\}_{n=1}^{N^{dof}}$ is an orthonormal basis of W_h with respect to $(\cdot, \cdot)_h$ such that for all $v \in W_h$ we have

$$a_h(w_h^{(n)}, v_h) = \lambda_h^{(n)}(w_h^{(n)}, v_h)_h.$$

2.1. Handling the non-linear term

Following [15], based on the properties of Π^0, for each element E in $\mathcal{T}_h$, we define $\tilde{f}(u_h)$ as:

$$\tilde{f}(u_h)|_E := \Pi^0(f(\Pi^0 u_h))|_E, \quad \text{for} \quad u_h \in W_h, \tag{11}$$

where we have the following orthogonal property

$$\int_E (\Pi^0 f - f) \, d\mathbf{x} = 0.$$

Now, with this definition, we have

$$(\tilde{f}(u_h), v_h) = \sum_{E\in\mathcal{T}_h} \int_E \Pi^0 f(\Pi^0 u_h)\cdot v_h \, d\mathbf{x} = \sum_{E\in\mathcal{T}_h} \int_E f(\Pi^0 u_h)\cdot \Pi^0 v_h \, d\mathbf{x}$$
$$= \sum_{E\in\mathcal{T}_h} \sum_{i=1}^{N_E^{dof}} f(u_{h,i}) \int_E \Pi^0\phi_i \cdot \Pi^0 v_h \, d\mathbf{x}, \tag{12}$$

where N_E^{dof} degrees of freedom for element E is considered and we used the Lagrangian type property for the canonical bases $\{\phi_i\}_{i=1}^{N^{dof}}$ for space W_h.

2.2 Fully-discrete scheme

In order to formulate the fully-discrete scheme for (10), a backward Euler method is employed to approximate the temporal variable t. First, we create a partition of time interval $[0,T]$ such that $0 = t_0 < t_1 < \cdots < t_M = T$ and $t_m = m\Delta t$ for $m = 0, 1, \cdots, M$ for the time step $\Delta t = T/M$. Therefore, the fully-discrete scheme can form in which: find $\mathcal{U}^n \approx u_h(\cdot, t_n) \in W_h$ such that

$$\begin{cases} (\frac{\mathcal{U}^n - \mathcal{U}^{n-1}}{\Delta t}, v_h)_h + a_h(\mathcal{U}^n, v_h) = (\tilde{f}(\mathcal{U}^n), v_h), \\ \mathcal{U}(\cdot, 0) = u_h^0. \end{cases} \tag{13}$$

By lagging the non-linear term, we can linearize the above problem as follows:

$$\begin{cases} (\frac{\mathcal{U}^n - \mathcal{U}^{n-1}}{\Delta t}, v_h)_h + a_h(\mathcal{U}^n, v_h) = (\tilde{f}(\mathcal{U}^{n-1}), v_h), \\ \mathcal{U}(\cdot, 0) = u_h^0, \end{cases} \tag{14}$$

where the non-linear term formed as $\tilde{f}(\mathcal{U}^{n-1}) = \mathcal{U}^{n-1}\nabla\cdot\mathcal{U}^n - \mathcal{U}^n(1-\mathcal{U}^{n-1})$.

3. Error analysis of discrete schemes

This section is devoted to error analyses for both semi-discrete and fully-discrete schemes in the related L^2 and H^1 norms. The section is divided into two subsections, where we investigate the errors between the exact solution u for the problem (1)-(3) and the corresponding approximate solutions for schemes (10) and (14), respectively. We employ the main tool from [18] throughout this process and denote a generic positive constant independent of the mesh size h by C.

We define the following mapping $\mathcal{P}_h : H_0^1(\Omega) \to W_h$ as the energy projection:

$$a_h(\mathcal{P}_h u, v_h) = a(u, v_h), \qquad \text{for} \qquad v_h \in W_h. \tag{15}$$

We have the following bounds for this projection.

Lemma 3.1. *Let $u \in H_0^1(\Omega)$. Then there exists a unique function $\mathcal{P}_h u \in W_h$ verifying*

$$|\mathcal{P}_h u - u|_1 \leq Ch^k |u|_{k+1}. \tag{16}$$

Moreover, if the domain Ω is convex, the following bound holds

$$\|\mathcal{P}_h u - u\|_0 \leq Ch^{k+1} |u|_{k+1}. \tag{17}$$

Proof. Refer to [18] for proof details. □

For $a, b \geq 0$ and $m \in \mathbb{N}$, we have

$$\frac{1}{2}(a+b)^2 \leq ma^2 + b^2. \tag{18}$$

3.1 Error analysis for semi-discrete scheme

As follows, we define the error equation for the difference of the solution of the problem (10) and the energy projection of the solution u for the problem (1)-(3) as:

$$e_h := u_h(\cdot, t) - \mathcal{P}_h u(\cdot, t).$$

Based on the introduced tools, we can provide an L^2-error estimate for the problem (10) as follows.

Theorem 3.2. *Let u be the solution of the continuous problem (1)-(3). For all $t \in [0, T]$, the following error estimate for the solution u_h of the problem (10) is hold*

$$\begin{aligned}\|u_h - u\|_0 \leq C\Big(&\|u_h(\cdot, 0) - u(\cdot, 0)\|_0 \\ &+ h^{k+1}(|u^0|_{k+1} + \|u(\cdot, t)\|_{L^2(0,t;H^{k+1}(\Omega))} + \|u_t(\cdot, t)\|_{L^1(0,t;H^{k+1}(\Omega))} \\ &+ \|u_t(\cdot, t)\|_{L^2(0,t;H^{k+1}(\Omega))} + \|f(u(\cdot, t))\|_{L^2(0,t;H^{k+1}(\Omega))})\Big).\end{aligned}$$

Proof. From the triangle inequality, we have

$$\|u_h - u\|_0 \leq \|e_h\|_0 + \|\mathcal{P}_h u - u\|_0. \tag{19}$$

Next, we proceed by bounding both terms on the right-hand side in (19) separately. From (17) we can easily write

$$\|\mathcal{P}_h u - u\|_0 \leq Ch^{k+1} |u|_{k+1} = Ch^{k+1}(|u^0|_{k+1} + \|u_t(\cdot, t)\|_{L^1(0,t;H^{k+1}(\Omega))}). \tag{20}$$

Multiplying both sides of Equation (1) by $v_h \in W_h$ and subtracting (10) from that, for all $t \in [0, T]$, yield

$$(\partial_t u_h - u_t, v_h)_h + a_h(u_h, v_h) = (\tilde{f}(u_h(\cdot, t)) - f(u(\cdot, t)), v_h) + a(u, v_h).$$

Then, by adding and subtracting terms $\frac{d}{dt}\mathcal{P}_h u$ and $\mathcal{P}_h u$ in the first and the second terms above, respectively, we will have

$$\begin{aligned}(\partial_t e_h, v_h)_h + a_h(e_h, v_h) &= (\tilde{f}(u_h(\cdot,t)) - f(u(\cdot,t)), v_h) \\ &+ a(u, v_h) - (\mathcal{P}_h u_t - u_t, v_h)_h - a_h(\mathcal{P}_h u, v_h) \\ &= (\tilde{f}(u_h(\cdot,t)) - f(u(\cdot,t)), v_h) \\ &+ a(u, v_h) - (\mathcal{P}_h u_t - u_t, v_h)_h - a(u, v_h) \text{ (by (15))} \\ &= (\tilde{f}(u_h(\cdot,t)) - f(u(\cdot,t)), v_h) \\ &- (\mathcal{P}_h u_t - u_t, v_h)_h, \end{aligned} \tag{21}$$

where we used the time derivative commutativity property with the energy projection. The next step involves bounding the two last terms in (21) separately. Inspired by [15] (Theorem 4.2), we will begin with the first term.

$$\begin{aligned}(\tilde{f}(u_h(\cdot,t)) - f(u(\cdot,t)), v_h) &= (\Pi^0 f(\Pi^0 u_h(\cdot,t)), v_h) \text{ (by (22))} \\ &- (\Pi^0 f(\Pi^0 u(\cdot,t)), v_h) + (\Pi^0 f(\Pi^0 u(\cdot,t)), v_h) \\ &- (\Pi^0 f(u(\cdot,t)), v_h) + (\Pi^0 f(u(\cdot,t)), v_h) \\ &- (f(u(\cdot,t)), v_h). \end{aligned} \tag{22}$$

From the Cauchy-Schwarz inequality, one can write

$$\begin{aligned}(\Pi^0 f(\Pi^0 u_h(\cdot,t)) - \Pi^0 f(\Pi^0 u(\cdot,t)), v_h) &\leq \|\Pi^0(f(\Pi^0 u_h(\cdot,t)) - f(\Pi^0 u(\cdot,t)))\|_0 \|v_h\|_0 \\ &\leq \|f(\Pi^0 u_h(\cdot,t)) - f(\Pi^0 u(\cdot,t))\|_0 \|v_h\|_0 \\ &\leq C\|\Pi^0 u_h(\cdot,t) - \Pi^0 u(\cdot,t))\|_0 \|v_h\|_0 \\ &\leq C\|u_h(\cdot,t) - u(\cdot,t))\|_0 \|v_h\|_0, \end{aligned} \tag{23}$$

where we used the fact that f is Lipschitz continuous together with boundedness property of the L^2-projection operator Π^0.

In a similar manner and using the error bound of L^2-projection operator Π^0, we will have

$$\begin{aligned}(\Pi^0 f(\Pi^0 u(\cdot,t)) - \Pi^0 f(u(\cdot,t)), v_h) &\leq \|\Pi^0(f(\Pi^0 u(\cdot,t)) - f(u(\cdot,t)))\|_0 \|v_h\|_0 \\ &\leq Ch^{k+1}|u(\cdot,t)|_{k+1}\|v_h\|_0. \end{aligned} \tag{24}$$

The error bound of L^2-projection operator Π^0 implies that

$$\begin{aligned}(\Pi^0 f(u(\cdot,t)) - f(u(\cdot,t)), v_h) &\leq \|\Pi^0 f(u(\cdot,t)) - f(u(\cdot,t))\|_0 \|v_h\|_0 \\ &\leq Ch^{k+1}|f(u(\cdot,t))|_{k+1}\|v_h\|_0. \end{aligned} \tag{25}$$

For the second term in (21), by using the Cauchy-Schwarz inequality and (17), we infer that

$$(\mathcal{P}_h u_t - u_t, v_h)_h \leq \|\mathcal{P}_h u_t - u_t\|_0 \|v_h\|_0 \leq Ch^{k+1}|u_t|_{k+1}\|v_h\|_0. \tag{26}$$

Considering (22)-(26) and setting $v_h = e_h$ in (21), we will have

$$\begin{aligned}(\partial_t e_h, e_h)_h + a_h(e_h, e_h) \\ \leq C\Big(\|u_h(\cdot,t) - u(\cdot,t)\|_0 + h^{k+1}(|u(\cdot,t)|_{k+1} \\ + |u_t(\cdot,t)|_{k+1} + |f(u(\cdot,t))|_{k+1})\Big)\|e_h\|_0.\end{aligned}$$

Using the fact that $a_h(e_h, e_h) = |e_h|_1^2 \geq 0$ and from (19), we have

$$\begin{aligned}\frac{1}{2}\frac{d}{dt}\|e_h\|_0^2 \leq C\Big(\|e_h\|_0 + \|\mathcal{P}_h u(\cdot,t) - u(\cdot,t)\|_0 \\ + h^{k+1}(|u(\cdot,t)|_{k+1} + |u_t(\cdot,t)|_{k+1} + |f(u(\cdot,t))|_{k+1})\Big)\|e_h\|_0.\end{aligned}$$

Integrating both sides of the above inequality from 0 to t, using the Young's inequality and (18), we infer that

$$\begin{aligned}\|e_h\|_0^2 - \|e_h(\cdot,0)\|_0^2 \leq C\Big(\int_0^t \|e_h(\cdot,s)\|_0^2 + \int_0^t \|\mathcal{P}_h u(\cdot,s) - u(\cdot,s)\|_0^2 \\ + h^{2k+2}(\|u(\cdot,t)\|^2_{L^2(0,t;H^{k+1}(\Omega))} \\ + \|u_t(\cdot,t)\|^2_{L^2(0,t;H^{k+1}(\Omega))} \\ + \|f(u(\cdot,t))\|^2_{L^2(0,t;H^{k+1}(\Omega))})\Big).\end{aligned}$$

Following the given idea for the Theorem 4.2 in [15], yields

$$\begin{aligned}\|e_h\|_0 \leq C\Big(\|u_h(\cdot,0) - u(\cdot,0)\|_0 + h^{k+1}(|u^0|_{k+1} \\ + \|u(\cdot,t)\|_{L^2(0,t;H^{k+1}(\Omega))} + \|u_t(\cdot,t)\|_{L^1(0,t;H^{k+1}(\Omega))} \\ + \|u_t(\cdot,t)\|_{L^2(0,t;H^{k+1}(\Omega))} + \|f(u(\cdot,t))\|_{L^2(0,t;H^{k+1}(\Omega))})\Big).\end{aligned} \tag{27}$$

Combining the estimates (20) and (27) with (19), we will have

$$\begin{aligned}\|u_h - u\|_0 \leq C\Big(\|u_h(\cdot,0) - u(\cdot,0)\|_0 + h^{k+1}(|u^0|_{k+1} \\ + \|u(\cdot,t)\|_{L^2(0,t;H^{k+1}(\Omega))} + \|u_t(\cdot,t)\|_{L^1(0,t;H^{k+1}(\Omega))} \\ + \|u_t(\cdot,t)\|_{L^2(0,t;H^{k+1}(\Omega))} + \|f(u(\cdot,t))\|_{L^2(0,t;H^{k+1}(\Omega))})\Big).\end{aligned}$$

We reached the desired result. □

We will now turn our attention to analyzing the H^1-error of the semi-discrete scheme (10).

Theorem 3.3. *Let u be the solution of the continues problem (1). For all $t \in [0,T]$, the following error estimate for the solution u_h of the problem (10) is hold*

$$\begin{aligned}|u_h - u|_1 \leq C\Big(&|u_h(\cdot,0) - u(\cdot,0)|_1 + h^k(|u^0|_{k+1} + \|u_t(\cdot,t)\|_{L^1(0,t;H^{k+1}(\Omega))}) \\ &+ h^{k+1}(\|u(\cdot,t)\|_{L^2(0,t;H^{k+1}(\Omega))} + \|u_t(\cdot,t)\|_{L^2(0,t;H^{k+1}(\Omega))} \\ &+ \|f(u(\cdot,t))\|_{L^2(0,t;H^{k+1}(\Omega))})\Big).\end{aligned}$$

Proof. From the triangle inequality, we have

$$|u_h - u|_1 \leq |e_h|_1 + |\mathcal{P}_h u - u|_1. \tag{28}$$

Based on the estimate (18), we immediately conclude that

$$|\mathcal{P}_h u - u|_1 \leq Ch^k|u|_{k+1} \leq Ch^k(\|u^0\|_{k+1} + \|u_t(\cdot,t)\|_{L^1(0,t;H^{k+1}(\Omega))}). \tag{29}$$

Setting $v_h = \partial_t e_h$ in (21), using the bounds (22)-(26) and (19), we have

$$\begin{aligned}(\partial_t e_h, \partial_t e_h)_h + a_h(e_h, \partial_t e_h) \leq C\Big(&\|e_h\|_0 + \|\mathcal{P}_h u(\cdot,t) + u(\cdot,t)\|_0 \\ &+ h^{k+1}(|u(\cdot,t)|_{k+1} + |u_t(\cdot,t)|_{k+1} \\ &+ |f(u(\cdot,t))|_{k+1})\Big)\|\partial_t e_h\|_0.\end{aligned}$$

Using the Young's inequality and from (18), we will have

$$\begin{aligned}(\partial_t e_h, \partial_t e_h)_h + a_h(e_h, \partial_t e_h) \leq C\Big(&\|e_h\|_0^2 + \|\mathcal{P}_h u(\cdot,t) - u(\cdot,t)\|_0^2 \\ &+ h^{2k+2}(|u(\cdot,t)|_{k+1}^2 + |u_t(\cdot,t)|_{k+1}^2 \\ &+ |f(u(\cdot,t))|_{k+1}^2)\Big) + \frac{\beta_*}{2}\|\partial_t u_h - \mathcal{P}_h u_t\|_0^2.\end{aligned}$$

From the stability property (9), we infer that

$$\begin{aligned}\beta_*\|\partial_t e_h\|_0^2 + \frac{\alpha_*}{2}\frac{d}{dt}|e_h|_1^2 \leq C\Big(&\|e_h\|_0^2 + \|\mathcal{P}_h u(\cdot,t) - u(\cdot,t)\|_0^2 \\ &+ h^{2k+2}(|u(\cdot,t)|_{k+1}^2 + |u_t(\cdot,t)|_{k+1}^2 + |f(u(\cdot,t))|_{k+1}^2)\Big).\end{aligned}$$

Because of $\|\partial_t e_h\|_0^2 \geq 0$, using the obtained estimates (20) and (27), from (18) and then integrating both sides from 0 to t, we can write

$$\begin{aligned}|e_h|_1^2 \leq C\Big(&|e_h(\cdot,0)|_1^2 + \|u_h(\cdot,0) - u(\cdot,0)\|_0^2 \\ &+ h^{2k+2}(|u^0|_{k+1}^2 + \|u(\cdot,t)\|_{L^2(0,t;H^{k+1}(\Omega))}^2 \\ &+ \|u_t(\cdot,t)\|_{L^2(0,t;H^{k+1}(\Omega))}^2 + \|f(u(\cdot,t))\|_{L^2(0,t;H^{k+1}(\Omega))}^2)\Big).\end{aligned} \tag{30}$$

We can estimate the first term in (30) as follows:

$$\begin{aligned}|e_h(\cdot,0)|_1 &\leq |u_h(\cdot,0)-u(\cdot,0)|_1 + |u(\cdot,0)-\mathcal{P}_h u(\cdot,0)|_1\\ &\leq |u_h(\cdot,0)-u(\cdot,0)|_1 + Ch^k|u^0|_{k+1}.\end{aligned}$$

Using the above estimate and from the Poincaré inequality, we have

$$\begin{aligned}|e_h|_1 \leq C\Big(&|u_h(\cdot,0)-u(\cdot,0)|_1 + h^k|u^0|_{k+1}\\ &+ h^{k+1}(\|u(\cdot,t)\|_{L^2(0,t;H^{k+1}(\Omega))} + \|u_t(\cdot,t)\|_{L^2(0,t;H^{k+1}(\Omega))}\\ &+ \|f(u(\cdot,t))\|_{L^2(0,t;H^{k+1}(\Omega))})\Big).\end{aligned}$$

Combining the above estimate and (29) with (28), we get the desired result. □

3.2 Error analysis for fully-discrete scheme

First, we introduce the error function between the numerical solution for the linearized fully-discrete scheme (14) and the energy projection of the solution u for the continuous problem (1)-(3) as follows:

$$e_h^n := \mathcal{U}^n - \mathcal{P}_h u(\cdot,t_n).$$

Theorem 3.4. *Let $u(\cdot,t_n)$ be the solution of the continuous problem (1)-(3) at time t_n. For $n=1,\cdots,N$, the following error estimate for the sequence $\{\mathcal{U}^n\}_{n=1}^N$ of the problem (14) is hold*

$$\begin{aligned}\|\mathcal{U}^n - u(\cdot,t_n)\|_0 \leq C\Big(&\|u_h^0 - u(\cdot,0)\|_0 + \Delta t(\|u_t\|_{L^1(0,t_n;L^2(\Omega))} + \|u_{tt}\|_{L^1(0,t_n;L^2(\Omega))})\\ &+ h^{k+1}(|u^0|_{k+1} + \|u_t\|_{L^1(0,t_n;H^{k+1}(\Omega))} + \max_{1\leq j\leq n}|u(\cdot,t_j)|_{k+1}\\ &+ \max_{1\leq j\leq n}|f(u(\cdot,t_j))|_{k+1})\Big).\end{aligned}$$

Proof. From the triangle inequality, we have

$$\|\mathcal{U}^n - u(\cdot,t_n)\|_0 \leq \|e_h^n\|_0 + \|\mathcal{P}_h u(\cdot,t_n) - u(\cdot,t_n)\|_0. \tag{31}$$

From (17), for the second term we infer that

$$\|\mathcal{P}_h u(\cdot,t_n) - u(\cdot,t_n)\|_0 \leq Ch^{k+1}|u(\cdot,t_n)|_{k+1}. \tag{32}$$

Following the same idea that is presented in Theorem 3.2, for the semi-discrete scheme (14) we will have

$$\begin{aligned}(\frac{e_h^n - e_h^{n-1}}{\Delta t}, v_h)_h + a_h(e_h^n, v_h) = &(\tilde{f}(\mathcal{U}^{n-1}) - f(u(\cdot,t_n)), v_h)\\ &+ (u_t(\cdot,t_n), v_h)\\ &- (\frac{\mathcal{P}_h u(\cdot,t_n) - \mathcal{P}_h u(\cdot,t_{n-1})}{\Delta t}, v_h)_h.\end{aligned} \tag{33}$$

Inspired by the idea in Theorem 3.2, we have the following bound

$$(\tilde{f}(\mathcal{U}^{n-1}) - f(u(\cdot,t_n)), v_h) \leq C\Big(\|\mathcal{U}^{n-1} - u(\cdot,t_n)\|_0 + h^{k+1}(|u(\cdot,t_n)|_{k+1} + |f(u(\cdot,t_n))|_{k+1})\Big)\|v_h\|_0. \tag{34}$$

On each element $E \in \mathcal{T}_h$, the following bound has been investigated in [18]

$$\begin{aligned}(u_t(\cdot,t_n), v_h) - (\frac{\mathcal{P}_h u(\cdot,t_n) - \mathcal{P}_h u(\cdot,t_{n-1})}{\Delta t}, v_h)_h \\ \leq \frac{C}{\Delta t}(\|\Delta t\, u_t(\cdot,t_n) - (u(\cdot,t_n) - u(\cdot,t_{n-1}))\|_0 \\ + h^{k+1}|u(\cdot,t_n) - u(\cdot,t_{n-1})|_{k+1})\|v_h\|_0 \\ =: \frac{C}{\Delta t}(\beta^n + \gamma^n)\|v_h\|_0.\end{aligned} \tag{35}$$

Using bounds (34) and (35), we can rewrite (33) as follows

$$\begin{aligned}(\frac{e_h^n - e_h^{n-1}}{\Delta t}, v_h)_h + a_h(e_h^n, v_h) \leq C\Big(\|\mathcal{U}^{n-1} - u(\cdot,t_n)\|_0 \\ + h^{k+1}(|u(\cdot,t_n)|_{k+1} + |f(u(\cdot,t_n))|_{k+1})\Big)\|v_h\|_0 \\ + \frac{C}{\Delta t}(\beta^n + \gamma^n)\|v_h\|_0.\end{aligned}$$

Setting $v_h = e_h^n$, from the stability property (9) and using the fact that $(e_h^n - e_h^{n-1}, e_h^n) \geq \|e_h^n\|_0^2 - \|e_h^{n-1}\|_0\|e_h^n\|_0$, for $n = 1, \cdots, N$ the above inequality can be written as

$$\begin{aligned}\|e_h^n\|_0 \leq C\Big((1+\Delta t)\|e_h^{n-1}\|_0 + \Delta t(\|\mathcal{P}_h u(\cdot,t_{n-1}) - u(\cdot,t_{n-1})\|_0 \\ + \|u(\cdot,t_{n-1}) - u(\cdot,t_n)\|_0 + h^{k+1}(|u(\cdot,t_n)|_{k+1} + |f(u(\cdot,t_n))|_{k+1}))\Big) \\ + C(\beta^n + \gamma^n) \\ =: C\|e_h^{n-1}\|_0 + C(\Delta t\,\alpha^n + \beta^n + \gamma^n).\end{aligned} \tag{36}$$

We claim that the following relation holds

$$\|e_h^n\|_0 \leq C\|e_h^0\|_0 + C\sum_{j=1}^{n}(\Delta t\,\alpha^j + \beta^j + \gamma^j). \tag{37}$$

In the following, we check the validity of our claim based on mathematical induction. For $n = 1$, the following relation is hold from (36)

$$\|e_h^1\|_0 \leq C\|e_h^0\|_0 + C(\Delta t\,\alpha^1 + \beta^1 + \gamma^1).$$

We assume that the following relation for $n = k$ holds

$$\|e_h^k\|_0 \leq C\|e_h^0\|_0 + C\sum_{j=1}^{k}(\Delta t\,\alpha^j + \beta^j + \gamma^j).$$

We are going to show that, for $n = k+1$ we have

$$\|e_h^{k+1}\|_0 \leq C\|e_h^0\|_0 + C\sum_{j=1}^{k+1}(\Delta t\,\alpha^j + \beta^j + \gamma^j).$$

From the original inequality (36), we can write

$$\|e_h^{k+1}\|_0 \leq C\|e_h^k\|_0 + C(\Delta t\,\alpha^{k+1} + \beta^{k+1} + \gamma^{k+1}).$$

According to the induction hypothesis, the desired relation (37) is achievable. Based on the obtained result, the relation (36) can be rewritten as:

$$\begin{aligned}\|e_h^n\|_0 \leq C\Big(&\|u_h^0 - u(\cdot,0)\|_0 + \Delta t\sum_{j=0}^{n}\|\mathcal{P}_h u(\cdot,t_j) - u(\cdot,t_j)\|_0 \\ &+ \Delta t\sum_{j=1}^{n}(\|u(\cdot,t_{j-1}) - u(\cdot,t_j)\|_0 + h^{k+1}(|u(\cdot,t_j)|_{k+1} + |f(u(\cdot,t_j))|_{k+1}))\Big) \\ &+ C\sum_{j=1}^{n}(\beta^j + \gamma^j). \end{aligned} \tag{38}$$

For the second term in (38), from (17) we can write

$$\begin{aligned}\Delta t\sum_{j=0}^{n}\|\mathcal{P}_h u(\cdot,t_j) - u(\cdot,t_j)\|_0 &\leq Ch^{k+1}\Delta t(|u^0|_{k+1} + \sum_{j=1}^{n}|u(\cdot,t_j)|_{k+1}) \\ &\leq Ch^{k+1}\Delta t(|u^0|_{k+1} + \sum_{j=1}^{n}\max_{1\leq j\leq n}|u(\cdot,t_j)|_{k+1}) \\ &= Ch^{k+1}\Delta t|u^0|_{k+1} + Ch^{k+1}n\Delta t\max_{1\leq j\leq n}|u(\cdot,t_j)|_{k+1} \\ &\leq Ch^{k+1}\Delta t|u^0|_{k+1} + Ch^{k+1}T\max_{1\leq j\leq n}|u(\cdot,t_j)|_{k+1}, \end{aligned} \tag{39}$$

and for the third term, we have

$$\begin{aligned}\sum_{j=1}^{n}\|u(\cdot,t_j) - u(\cdot,t_{j-1})\|_0 &= \sum_{j=1}^{n}\|\int_{t_{j-1}}^{t_j} u_t(\cdot,s)\,ds\|_0 \\ &\leq \sum_{j=1}^{n}\int_{t_{j-1}}^{t_j}\|u_t(\cdot,s)\|_0\,ds = \int_0^{t_n}\|u_t(\cdot,s)\|_0\,ds \\ &= \|u_t\|_{L^1(0,t_n;L^2(\Omega))}. \end{aligned} \tag{40}$$

The following bounds for the rest of terms in (36) have been investigated in [15, 18]

- $$h^{k+1}\Delta t\sum_{j=1}^{n}|u(\cdot,t_j)|_{k+1} \le h^{k+1}n\Delta t \max_{1\le j\le n}|u(\cdot,t_j)|_{k+1}$$
$$\le h^{k+1}T \max_{1\le j\le n}|u(\cdot,t_j)|_{k+1} \quad (n\Delta t = n\frac{T}{N} \le T), \tag{41}$$

- $$h^{k+1}\Delta t\sum_{j=1}^{n}|f(u(\cdot,t_j))|_{k+1} \le h^{k+1}T \max_{1\le j\le n}|f(u(\cdot,t_j))|_{k+1}, \tag{42}$$

- $$\sum_{j=1}^{n}(\beta^j+\gamma^j) \le \Delta t\|u_{tt}\|_{L^1(0,t_n;L^2(\Omega))} + h^{k+1}\|u_t\|_{L^1(0,t_n;H^{k+1}(\Omega))}. \tag{43}$$

Substituting (39)-(43) in (38), we will have

$$\|e_h^n\|_0 \le C\Big(\|u_h^0 - u(\cdot,0)\|_0 + \Delta t(\|u_t\|_{L^1(0,t_n;L^2(\Omega))} + \|u_{tt}\|_{L^1(0,t_n;L^2(\Omega))})$$
$$+ h^{k+1}(|u^0|_{k+1} + \|u_t\|_{L^1(0,t_n;H^{k+1}(\Omega))} + \max_{1\le j\le n}|u(\cdot,t_j)|_{k+1}$$
$$+ \max_{1\le j\le n}|f(u(\cdot,t_j))|_{k+1})\Big).$$

Combining the above inequality with (32), gives us the desired result. □

4. Formulation details

Here, based on the fully-discrete scheme (14), some details are provided for better understanding of the algorithm. For a set of bases $\{\phi_i\}_{i=1}^{N^{dof}}$, any solution $u_h \in W_h$ can represent as:

$$u_h = \sum_{i=1}^{N^{dof}} u_{h,i}\,\phi_i.$$

From (14) for $v_h = \phi_j$, we have

$$\sum_{i=1}^{N^{dof}} u_{h,i}^n(\phi_i,\phi_j)_{\mathcal{T}_h} + \Delta t\sum_{i=1}^{N^{dof}} u_{h,i}^n a_h(\phi_i,\phi_j) = \Delta t(\tilde{f}(\sum_{i=1}^{N^{dof}} u_{h,i}^{n-1}\,\phi_i),\phi_j)_{\mathcal{T}_h}$$
$$+ \sum_{i=1}^{N^{dof}} u_{h,i}^{n-1}\,(\phi_i,\phi_j)_{\mathcal{T}_h}, j = 1,\cdots,N^{dof}, \tag{44}$$

where the first term on the right-hand side in (44) will be formed from (12) as:

$$
\begin{aligned}
(\tilde{f}(\sum_{i=1}^{N^{dof}} u_{h,i}^{n-1}\,\phi_i),\phi_j)_{\mathcal{T}_h} &= (\Pi^0 f(\sum_{i=1}^{N^{dof}} u_{h,i}^{n-1}\,\Pi^0\phi_i),\phi_j)_{\mathcal{T}_h} \\
&= (f(\sum_{i=1}^{N^{dof}} u_{h,i}^{n-1}\,\Pi^0\phi_i),\Pi^0\phi_j)_{\mathcal{T}_h} \\
&= (\sum_{i=1}^{N^{dof}} u_{h,i}^{n-1}\,\Pi^0\phi_i(\sum_{i=1}^{N^{dof}} u_{h,i}^{n}\,\nabla\cdot\Pi^0\phi_i),\Pi^0\phi_j)_{\mathcal{T}_h} \\
&- (\sum_{i=1}^{N^{dof}} u_{h,i}^{n}\,\Pi^0\phi_i(1-\sum_{i=1}^{N^{dof}} u_{h,i}^{n-1}\,\Pi^0\phi_i),\Pi^0\phi_j)_{\mathcal{T}_h}.
\end{aligned}
$$

5. Numerical simulation

In this section, to show the efficiency and accuracy of the introduced algorithm, we apply the proposed technique to numerical simulation of the model problem (1)-(3) with $\alpha = 1$. Numerical outcomes show that our algorithm can achieve the optimal order of convergence, where this order is based on change of the degree of our virtual space. We carry out our numerical calculations using MATLAB R2022b and performed on a Laptop computer with 16.0 GB memory and Intel(R) Core(TM) i7-11800H CPU 2.30GHz.

To achieve our goal, we follow some basic steps:

- We start by partitioning our spatial domain Ω into convex and non-convex elements, and then create subintervals of the time interval $[0, 1]$ with a specific time step Δt.

- The initial and boundary conditions have been chosen in such a way that the exact solution for the problem (1)-(3) is as follows:

$$u(\mathbf{x}, t) = t\sin(\pi x)\sin(\pi y). \tag{45}$$

- By lagging the non-linear term and using the L^2-projection Π^0, this term will be handled in an interesting way.

- Based on different number of elements (for both convex and non-convex decomposition), we present L^2 ($\|e_h\|_0$) and H^1 ($\|e_h\|_1$) errors for $k = 1$ and

$k = 2$ where the related errors will be computed using the following functions

$$\|e_h\|_0 = \sqrt{\sum_{E\in\mathcal{T}_h} \|u - \Pi^0 u_h\|^2_{L^2(E)}},$$
$$|e_h|_1 = \sqrt{\sum_{E\in\mathcal{T}_h} |u - \Pi^\nabla u_h|^2_{H^1(E)}}.$$

The related L^2 and H^1 errors between the exact solution and the numerical solution for $k = 1, 2$ and $\Delta t = 0.01$ on a computational domain decomposition, contains convex and non-convex elements, are reported when taking into consideration the exact solution (45). In Figure 1, the number of degrees of freedom for both convex and non-convex elements for different values of k is depicted, and as expected, there are more degrees of freedom on the non-convex element.

From Table 1, one can observe that by increasing the number of elements on a convex decomposition, the related error will decrease. The numerical outcomes show that by changing the order of the polynomial space from 1 to 2, the convergence rate for both L^2 and H^1 norms will increase. For $k = 1$ and $k = 2$, the convergence rate in L^2 norm is 2 and 3, respectively and the convergence rate in H^1 norm is 1 and 2, respectively. These results show the efficiency of the proposed algorithm and satisfy the theory presented in the previous sections.

In Table 2, the computational error in both L^2 and H^1 norms between the exact solution and the numerical solution is analyzed. For $k = 1$ and $k = 2$, the numerical errors on non-convex mesh with different number of elements are reported in which one can infer that by increasing the number of elements, the related error will decrease. By going from $k = 1$ to $k = 2$, the convergence rate in L^2 and H^1 norms will increase. Based on these outcomes, for $k = 1$ and $k = 2$, the rate of convergence is 2 and 3 in L^2 norm, respectively and in H^1 norm, the rate of convergence is 1 and 2, respectively. We can infer that the presented theory in the previous sections will satisfy.

In Figure 2, a visualization for both convex (100 elements) and non-convex (256 elements) spatial domain decomposition is depicted. A $3D$ comparison between the exact solution and the numerical solution for $k = 1$ and $\Delta t = 0.01$ on a non-convex mesh (with 256 elements) is established in Figure 3. As our main goal of this paper, we compared FEM and VEM in solving the model problem (1)-(3). Both FEM and VEM used first-order polynomials in their respective approximation spaces for this comparison. As we mentioned before, the main difference between these two methods is that, unlike FEM, no computation of the shape functions is required. For $\alpha = 1$ and $\Delta t = 0.01$, we investigated the simulation process on convex spatial domain decomposition. Both methods can achieve the same order of convergence. A comparison of the computation time processes for FEM and VEM is shown in Figure 4. It is clear that the FEM requires less computation time than the VEM, but it should be noted that using the FEM to solve model problems presents some challenges when dealing with non-convex domain decomposition [19, 20].

Table 1: L^2 and H^1 errors and convergence rates for $k = 1, 2$ on convex mesh.

k	***elements***	$\|e_h\|_0$	***Rate***	$\|e_h\|_1$	***Rate***
	100	$1.4985e-03$	–	$1.2234e-02$	–
	400	$3.7696e-04$	1.99	$6.1566e-03$	0.99
1	1600	$9.4402e-05$	2.00	$3.0840e-03$	1.00
	6400	$2.3611e-05$	2.00	$1.5428e-03$	1.00
	100	$1.0998e-04$	–	$9.1600e-04$	–
	400	$1.3858e-05$	2.99	$2.3556e-04$	1.96
2	1600	$1.8029e-06$	2.94	$6.3308e-05$	1.90
	6400	$2.2641e-07$	2.99	$1.5948e-05$	1.99

Table 2: L^2 and H^1 errors and convergence rates for $k = 1, 2$ on non-convex mesh.

k	***elements***	$\|e_h\|_0$	***Rate***	$\|e_h\|_1$	***Rate***
	16	$1.0670e-02$	–	$2.7731e-02$	–
	64	$3.0418e-03$	1.81	$1.3756e-02$	1.01
1	256	$7.8915e-04$	1.95	$6.9135e-03$	0.99
	1024	$2.0018e-04$	1.98	$3.4802e-03$	0.99
	16	$2.1160e-03$	–	$4.1689e-03$	–
	64	$3.0715e-04$	2.78	$1.0783e-03$	1.95
2	256	$4.0435e-05$	2.93	$2.7235e-04$	1.99
	1024	$5.1377e-06$	2.98	$6.8564e-05$	1.99

6. Conclusion

In this paper, a generalized version of FEM that is called VEM is introduced and applied to a combined Burgers-Fisher equation. VEM gives us some powerful instruments that we handled the non-linearity term occurred in the model equation by them. The backward Euler scheme is used to approximate the derivative of the temporal variable. To show the efficiency and flexibility of our numerical scheme, we employed our algorithm on convex and non-convex meshes. The numerical outcomes show that our algorithm is sensitive to the degree of the computational space in which, by increasing the order of the polynomial space, the rate of convergence of the algorithm will increase. We presented a comparison between FEM and VEM. As depicted, the FEM has less computation time than the VEM. Also, we concluded that the VEM is more flexible than the FEM when dealing with non-convex domain decomposition.

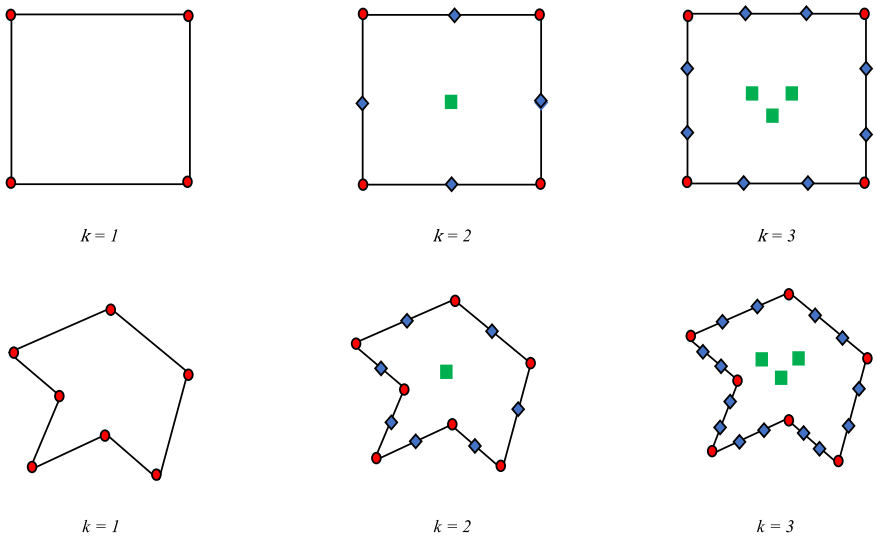

Figure 1: Number of degrees of freedom for different values of k, both convex (top row) and non-convex (bottom row).

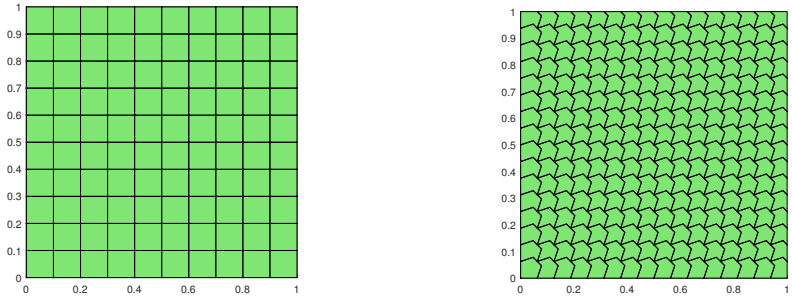

Figure 2: Visualization for the convex (left panel) and non-convex (right panel) spatial domain decomposition.

Conflicts of Interest. The authors declare that they have no conflicts of interest regarding the publication of this article.

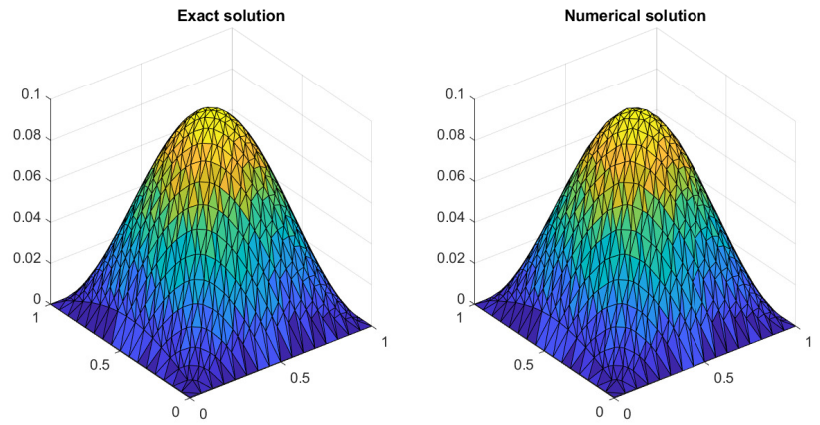

Figure 3: Comparison between exact and numerical solution for $k = 1$ and $\Delta t = 0.01$ on non-convex mesh.

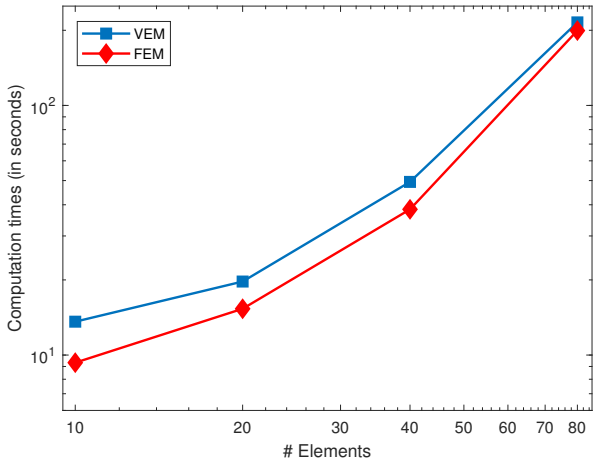

Figure 4: FEM and VEM computation time comparison.

References

[1] R. A. Fisher, The wave of advance of advantageous genes, *Ann. Eugen.* **7** (1937) 355 – 369, https://doi.org/10.1111/j.1469-1809.1937.tb02153.x.

[2] J. E. Macías-Díaz and A. E. González, A convergent and dynamically consistent finite-difference method to approximate the positive and bounded solu-

tions of the classical Burgers-Fisher equation, *J. Comput. Appl. Math.* **318** (2017) 604 − 615, https://doi.org/10.1016/j.cam.2015.11.018.

[3] P. Ladeveze and D. Leguillon, Error estimate procedure in the finite element method and applications, *SIAM J. Numer. Anal.* **20** (1983) 485 − 509, https://doi.org/10.1137/0720033.

[4] O. P. Yadav and R. Jiwari, Finite element analysis and approximation of Burgers-Fisher equation, *Numer. Methods Partial Differential Equations* **33** (2017) 1652 − 1677, https://doi.org/10.1002/num.22158.

[5] A. Yazdani, N. Mojahed, A. Babaei and E. V. Cendon, Using finite volume-element method for solving space fractional advection-dispersion equation, *Prog. Fract. Differ. Appl.* **6** (2020) 55 − 66, http://dx.doi.org/10.18576/pfda/060106.

[6] P. F. Antonietti, G. Manzini and M. Verani, The conforming virtual element method for polyharmonic problems, *Comput. Math. Appl.* **79** (2020) 2021 − 2034, https://doi.org/10.1016/j.camwa.2019.09.022.

[7] D. van Huyssteen and B. D. Reddy, The incorporation of mesh quality in the stabilization of virtual element methods for nonlinear elasticity, *Comput. Methods Appl. Mech. Engrg.* **392** (2022) p. 114720, https://doi.org/10.1016/j.cma.2022.114720.

[8] M. Li, Cut-off error splitting technique for conservative nonconforming VEM for N-coupled nonlinear Schrödinger-Boussinesq equations, *J. Sci. Comput.* **93** (2022) p. 86, https://doi.org/10.1007/s10915-022-02050-z.

[9] M. Li, L. Wang and N. Wang, Variable-time-step BDF2 nonconforming VEM for coupled Ginzburg-Landau equations, *Appl. Numer. Math.* **186** (2023) 378 − 410, https://doi.org/10.1016/j.apnum.2023.01.022.

[10] S. Berrone, A. Borio and G. Manzini, SUPG stabilization for the nonconforming virtual element method for advection-diffusion-reaction equations, *Comput. Methods Appl. Mech. Eng.* **340** (2018) 500 − 529, https://doi.org/10.1016/j.cma.2018.05.027.

[11] L. Beirão da Veiga, K. Lipnikov and G. Manzini, Arbitrary-order nodal mimetic discretizations of elliptic problems on polygonal meshes, *SIAM J. Numer. Anal.* **49** (2011) 1737 − 1760, https://doi.org/10.1137/100807764.

[12] F. Brezzi, K. Lipnikov and M. Shashkov, Convergence of the mimetic finite difference method for diffusion problems on polyhedral meshes, *SIAM J. Numer. Anal.* **43** (2005) 1872 − 1896, https://doi.org/10.1137/040613950.

[13] L. Beirão da Veiga, F. Brezzi, A. Cangiani, G. Manzini, L. D. Marini and A. Russo, Basic principles of virtual element methods, *Math. Models Methods Appl. Sci.* **23** (2013) 199 − 214, https://doi.org/10.1142/S0218202512500492.

[14] L. Beirão da Veiga, F. Brezzi, L. D. Marini and A. Russo, The hitchhiker's guide to the virtual element method, *Math. Models Methods Appl. Sci.* **24** (2014) 1541 – 1573, https://doi.org/10.1142/S021820251440003X.

[15] D. Adak, E. Natarajan and S. Kumar, Convergence analysis of virtual element methods for semilinear parabolic problems on polygonal meshes, *Numer. Methods Partial Differential Equations* **35** (2019) 222 – 245, https://doi.org/10.1002/num.22298.

[16] M. Li, J. Zhao, C. Huang and S. Chen, Nonconforming virtual element method for the time fractional reaction-subdiffusion equation with non-smooth data, *J. Sci. Comput.* **81** (2019) 1823 – 1859, https://doi.org/10.1007/s10915-019-01064-4.

[17] M. Li, J. Zhao, C. Huang and S. Chen, Conforming and nonconforming VEMs for the fourth-order reaction-subdiffusion equation: a unified framework, *IMA J. Numer. Anal.* **42** (2022) 2238 – 2300, https://doi.org/10.1093/imanum/drab030.

[18] G. Vacca and L. Beirão da Veiga, Virtual element methods for parabolic problems on polygonal meshes, *Numer. Methods Partial Differential Equations* **31** (2015) 2110 – 2134, https://doi.org/10.1002/num.21982.

[19] H. Chi, C. Talischi, O. Lopez-Pamies and G. H. Paulino, Polygonal finite elements for finite elasticity, *Int. J. Numer. Methods Eng.* **101** (2015) 305 – 328, https://doi.org/10.1002/nme.4802.

[20] S. W. Wu, G. R. Liu, C. Jiang, X. Liu, K. Liu, D. T. Wan and J. H. Yue, Arbitrary polygon mesh for elastic and elastoplastic analysis of solids using smoothed finite element method, *Comput. Methods Appl. Mech. Eng.* **405** (2023) p. 115874, https://doi.org/10.1016/j.cma.2022.115874.

Allahbakhsh Yazdani Cherati
Department of Applied Mathematics,
Faculty of Mathematical Sciences,
University of Mazandaran,
Babolsar, I. R. Iran
e-mail: yazdani@umz.ac.ir

Hamid Momeni
Department of Applied Mathematics,
Faculty of Mathematical Sciences,
University of Mazandaran,
Babolsar, I. R. Iran
e-mail: H.momeni07@umail.umz.ac.ir